Two-dimensional Hubbard model with nearest- and next-nearest-neighbor hopping

H. Q. Lin and J. E. Hirsch
Department of Physics, University of California, San Diego, La Jolla, California 92093
(Received 19 May 1986)

We study the magnetic properties of the two-dimensional Hubbard model with nearest-neighbor (t) and next-nearest-neighbor (t_2) hopping and on-site repulsion U. We first calculate the mean-field phase diagram as a function of band filling and U. Because of the Van Hove singularity in the density of states, we find a ferromagnetic phase extending to zero U for certain band filling. For the half-filled band case, antiferromagnetism sets in at a finite value of U if $t_2 \neq 0$. We study the behavior of spin-spin correlation functions for small lattices of up to $N=64$ atoms using Monte Carlo simulations, as well as exact diagonalization for $N=4$. Our results show enhanced ferromagnetic correlations in some regions, but apparently no ferromagnetic long-range order. In the half-filled case, our numerical results are consistent with a nonzero critical U. For a non-half-filled band our results suggest that there is no long-range order.

I. INTRODUCTION

A simple model to describe the main features of electron correlations in narrow energy bands is the Hubbard model,[1-3] defined by the Hamiltonian:

$$H=\sum_{\substack{i,j=1\\ \sigma}}^{N} t_{ij}C_{i\sigma}^{\dagger}C_{j\sigma}+U\sum_{i=1}^{N} n_{i\uparrow}n_{i\downarrow}-\mu\sum_{i=1}^{N}(n_{i\uparrow}+n_{i\downarrow}) , \tag{1.1}$$

which describes a single s band in a tight-binding basis, with a repulsive Coulomb interaction between electrons with opposite spin at the same atomic orbital. In Eq. (1.1), $C_{i\sigma}^{\dagger}(C_{i\sigma})$ is the creation (annihilation) operator for spin $\sigma=\uparrow,\downarrow$ at site i, and $n_{i\sigma}=C_{i\sigma}^{\dagger}C_{i\sigma}$, μ is the chemical potential, and t_{ij} is the hopping term defined by the overlap integral

$$t_{ij}=-\int d^3r\Phi_i^*(\mathbf{r})\Delta V(\mathbf{r})\Phi_j(\mathbf{r}-\mathbf{R}) , \tag{1.2}$$

where $\mathbf{R}=\mathbf{r}_i-\mathbf{r}_j$, and $\Delta V(\mathbf{r})$ contains all corrections to the atomic potential required to produce the full periodic crystal potential. The properties of the model are sensitive to the band structure, and most studies of the Hubbard model have considered nearest-neighbor hopping only.[4-8] We consider here the model on a two-dimensional square lattice. In the case of nearest-neighbor hopping only, and for the half-filled band case, its properties are determined by two distinct features of the model: nesting of the Fermi surface, and the logarithmic singularity in the density of states at the Fermi energy.[8] The logarithmic singularity in the density of states always occurs in two dimensions because of topology, but nesting of the Fermi surface will be absent if we change the band structure by including next-nearest-neighbor hopping. Since in the tight-binding picture the atomic wave functions are well localized, the magnitude of the hopping t_{ij} decreases rapidly with distance $|\mathbf{r}_i-\mathbf{r}_j|$. Here we restrict ourselves to nearest- and next-nearest-neighbor hopping.

$$t_{ij}=\begin{cases}-t & \text{if } i,j \text{ are nearest neighbor,}\\ t_2 & \text{if } i,j \text{ are next nearest neighbor,}\\ 0 & \text{otherwise.}\end{cases} \tag{1.3}$$

In the following we set $t=1$ and $0<t_2/t<0.5$ is always assumed.

The energy band for the noninteracting case ($U=0$) is

$$e_{\mathbf{k}}=4t_2\cos k_x\cos k_y-2t(\cos k_x+\cos k_y)-\mu , \tag{1.4}$$

$$\mathbf{k}_{x,y}=\frac{2\pi}{N_{x,y}}n_{x,y};\quad -\frac{N_{x,y}}{2}\le n_{x,y}<\frac{N_{x,y}}{2} \tag{1.5}$$

so that the bandwidth is $W=8t$.

The purpose of this paper is to study the effect of t_2 on the magnetic properties of the model. In the following section we discuss some features of this effect in the Hartree-Fock approximation. In Sec. III we present some results of computer simulations on lattices up to 64 sites for the half-filled case, and in Sec. IV we discuss the possibility of ferromagnetism in non-half-filled-band cases. Finally, we summarize our conclusions in Sec. V.

II. MEAN-FIELD SOLUTIONS

In this section we discuss the phase boundary obtained from mean-field calculations. The mean-field Hamiltonian is

$$H_{\mathrm{HF}}=\sum_{\substack{i,j=1\\ \sigma}}^{N} t_{ij}C_{i\sigma}^{\dagger}C_{j\sigma}-\mu\sum_{\substack{i=1\\ \sigma}}^{N} n_{i\sigma}+U\sum_{i=1}^{N}(\langle n_{i\uparrow}\rangle n_{i\downarrow}+n_{i\uparrow}\langle n_{i\downarrow}\rangle-\langle n_{i\uparrow}\rangle\langle n_{i\downarrow}\rangle) . \tag{2.1}$$

We consider three possible solutions.

(i) Paramagnetic state. For this state, we have the following self-consistent equation:

$$\langle n_{i\uparrow}\rangle=\langle n_{i\downarrow}\rangle=\tfrac{1}{2}n=\frac{1}{N}\sum_{\mathbf{k}} f(E_{\mathbf{k}}) \tag{2.2}$$

and the total energy is

$$\langle H_{\rm HF}\rangle = \sum_{k\sigma} E_k f(E_k) - \frac{U}{N}\langle n_\uparrow\rangle\langle n_\downarrow\rangle$$
$$= 2\sum_k E_k f(E_k) - \tfrac{1}{4}UNn^2 , \quad (2.3)$$

where n is the average number of electrons per atom and $E_k = e_k + Un$ with the band energy e_k given by Eq. (1.3). $f(e) = 1/[1+\exp(\beta e)]$ is the ordinary Fermi-Dirac function.

(ii) Ferromagnetic state. The self-consistent equations are

$$\langle n_{i\uparrow}\rangle = \tfrac{1}{2}n + x , \quad (2.4a)$$
$$\langle n_{i\downarrow}\rangle = \tfrac{1}{2}n - x , \quad (2.4b)$$
$$\langle n_\sigma\rangle = \frac{1}{N}\sum_k f(E_{k\sigma}) , \quad (2.4c)$$
$$E_{k\sigma} = e_k + U\langle n_{-\sigma}\rangle , \quad (2.4d)$$

and the total energy is

$$\langle H_{\rm HF}\rangle = \sum_{k\sigma} E_{k\sigma} f(E_k) - UN\langle n_\uparrow\rangle\langle n_\downarrow\rangle . \quad (2.5)$$

(iii) Antiferromagnetic state. Suppose that

$$\langle n_{i\uparrow}\rangle = \tfrac{1}{2}n + (-1)^{i_x+i_y}m , \quad (2.6a)$$
$$\langle n_{i\downarrow}\rangle = \tfrac{1}{2}n - (-1)^{i_x+i_y}m . \quad (2.6b)$$

By using the Fourier transform $C_{i\sigma} = (1/\sqrt{N})\sum_k a_{k\sigma} e^{-ik\cdot r_i}$, the Hamiltonian can be written as

$$H_{\rm HF} = \sum_{\substack{i,j=1\\ \sigma}}^{N} t_{ij} C_{i\sigma}^\dagger C_{j\sigma} - (\mu - \tfrac{1}{2}Un)\sum_{\substack{i=1\\ \sigma}}^{N} n_{i\sigma}$$
$$+ UN(m^2 - \tfrac{1}{4}n^2) + Um\sum_{i=1}^{N}(-1)^{i_x+i_y}(n_{i\uparrow} - n_{i\downarrow})$$
$$= H_\uparrow + H_\downarrow + UN(m^2 - \tfrac{1}{4}n^2) , \quad (2.7)$$

where

$$H_\sigma = \sum_k (e_k + \tfrac{1}{2}Un)n_{k\sigma} - \sigma Um\sum_k a_{k\sigma}a_{k+\pi\sigma} \equiv \sum_{\{k\}} H_{k\sigma} , \quad (2.8a)$$

$$H_{k\sigma} = (e_k + \tfrac{1}{2}Un)n_{k\sigma} + (e_{k+\pi} + \tfrac{1}{2}Un)n_{k+\pi\sigma} - \sigma Um(a_{k\sigma}^+ a_{k+\pi\sigma} + a_{k+\pi\sigma}^+ a_{k\sigma}) , \quad (2.8b)$$

with the set of $\{k\}$'s belonging to half of the original Brillouin zone enclosed by $|k_x \pm k_y| = \pi$. Hence the self-consistent equations determining m and μ are

$$n = \sum_{\{k\}}[f(E_k^+) + f(E_k^-)] , \quad (2.9a)$$
$$m = \frac{Um}{N}\sum_{\{k\}} \frac{[f(E_k^-) - f(E_k^+)]}{\{[\frac{1}{2}(e_k - e_{k+\pi})]^2 + U^2m^2\}^{1/2}} , \quad (2.9b)$$

where

$$E_k^\pm = \tfrac{1}{2}Un + \tfrac{1}{2}(e_k + e_{k+\pi})$$
$$\pm\{[\tfrac{1}{2}(e_k - e_{k+\pi})]^2 + U^2m^2\}^{1/2}$$
$$= \tfrac{1}{2}Un - \mu + 4t_2\cos k_x\cos k_y$$
$$\pm\{[2t(\cos k_x + \cos k_y)]^2 + U^2m^2\}^{1/2} .$$

By comparing energies in these three different states we can determine the ground state and hence the phase diagram for given interaction U and band filling n (there could be other kinds of ground states such as a ferromagnetic state which are not considered here). Another way to obtain the phase diagram is through the use of response functions.[5] This method enables one to test the relative stability of the different phases. We examine the sign of the z component of the paramagnetic susceptibility $\chi_z(q)$ (the system is rotational invariant in spin space) for $q=0$ and $q=\pi$. The susceptibility $\chi_z(q)$ is given by

$$\chi_z(q) = \frac{2\mu_B^2\Gamma(q)}{1 - U\Gamma(q)} , \quad (2.10a)$$

where

$$\Gamma(q) = -\frac{1}{N}\sum_k \left[\frac{f(e_{k+q}) - f(e_k)}{e_{k+q} - e_k}\right] . \quad (2.10b)$$

For $q=0$ we have

$$\Gamma(0) = \lim_{q\to 0}\Gamma(q) = \frac{1}{N}\sum_k \frac{\partial f(e_k)}{\partial e_k}$$
$$= \frac{1}{N}\sum_k \delta(e_k - \mu) = \rho(\mu) , \quad (2.11)$$

where $\rho(\mu)$ is the single-particle density of state at the Fermi level. So the instability criterion is $U\rho(\mu) = 1$ (Stoner criterion), such that for $U < 1/\rho(\mu)$ the paramagnetic state is stable with respect to the ferromagnetic state. For $q = \pi(1,1)$ we have

$$\Gamma(\pi) = -\frac{1}{N}\sum_k \frac{f(e_{k+\pi}) - f(e_k)}{e_{k+\pi} - e_k} \quad (2.12)$$

and in the particular case of $t_2 = 0$, one has $e_{k+\pi} = -e_k$ so that $\Gamma(\pi) = \int_{-4t}^{\mu} d\epsilon[\rho(\epsilon)/\epsilon]$. The equation $U = 1/\Gamma(\pi)$ determines the phase boundary between paramagnetic and antiferromagnetic states. Similarly, one can determine the phase boundary between ferromagnetic and antiferromagnetic states. Both the energy-comparison method and the response-function method are consistent and the phase diagrams for $t_2 = 0.2$ and $t_2 = 0.4$ are presented in Fig. 1. Two important features arise when we turn on next-nearest-neighbor hopping. One is the competition between antiferromagnetism and ferromagnetism at chemical potential $\mu = -4t_2$ where the density of states diverges logarithmically. The other one is that the transition between paramagnetic and antifer-

romagnetic states occurs at a nonzero value of U for the half-filled band case rather than at $U=0$ as for $t_2=0$.

A. Ferromagnetism versus antiferromagnetism at $\mu=-4t_2$

The Fermi surfaces at different band filling and the density of states for different hoppings t_2 are shown in Figs. 2 and 3. The straight line $|k_x \pm k_y| = \pi$ corresponds to the $t_2=0$ case. For the antiferromagnetic state ($\mathbf{q}=\pi$), the summands in Eq. (2.10b) with (k_x,k_y) are such that $|k_y \pm k_y| = \pi$ are singular. When $t_2=0$, the set of singular points coincides with the magnetic zone boundary because of nesting, but it consists only of four points $k_x=0$, $k_y=\pm\pi$; $k_x=\pm\pi$, $k_y=0$ whenever $t_2>0$, so that we expect the integral to be finite because the measure of the set of singular points is zero. To be more explicit, let us expand the energy band $e_{\mathbf{k}}$ in the vicinity of the saddle point $k_x=-\pi$, $k_y=0$, for example, as shown in Fig. 2(b):

$$\begin{aligned} e_{\mathbf{k}} &= -2t[-\cos(k_x-\pi)+\cos(k_y)] \\ &\quad -4t_2\cos(k_x-\pi)\cos(k_y)-\mu \\ &= r_y^2 - r_x^2 - 4t_2 + 2t_2(r_x^2+r_y^2) - \mu + O(r^4) \\ &= r^2(\sin^2\theta - \cos^2\theta + 2t_2) - 4t_2 - \mu + O(r^4) , \end{aligned} \tag{2.13}$$

where $r_x=k_x-\pi$, $r_y=k_y$ and we have used polar coordinates. Let $x=\mu+4t_2<0$, then the condition $e_{\mathbf{k}}<0$ becomes $\cos(2\theta)+2t_2<x/r<0$ so that the maximum angle of θ is

$$\theta_0=(\tfrac{1}{2})\cos^{-1}(2t_2-x)<(\tfrac{1}{2})\cos^{-1}(2t_2)$$

(we assume $t_2<0.5$). Since those four saddle points are equivalent, $\Gamma(\pi)$ becomes

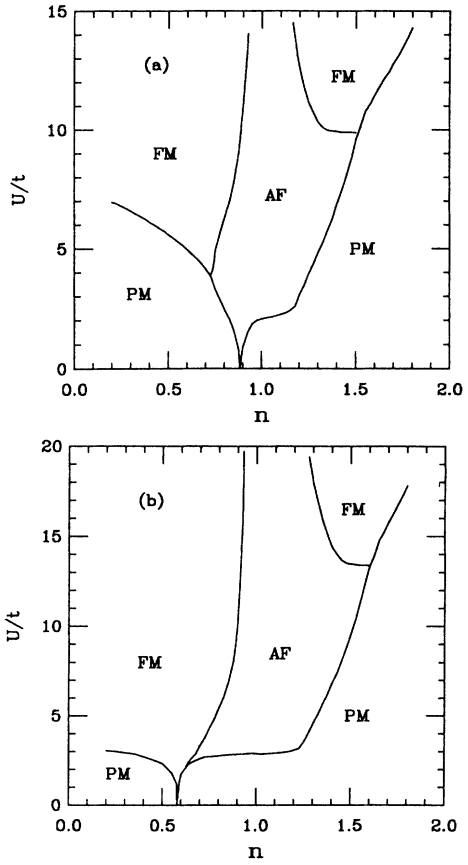

FIG. 1. The Hartree-Fock phase diagram for two-dimensional Hubbard model with nearest- and next-nearest-neighbor hopping. (a) $t_2=0.2$, and (b) $t_2=0.4$.

$$\begin{aligned} \Gamma(\pi) &= \frac{4}{(2\pi)^2} 4 \int_0^{\theta_0} \frac{d\theta}{2\cos(2\theta)} \int_{r(\theta)}^{r_0} \frac{r\,dr}{r^2} \\ &= \frac{8}{(2\pi)^2} \int_0^{\theta_0} \frac{d\theta}{\cos(2\theta)} \left[\ln\left|\frac{r_0}{x}\right| + \ln|2t_2 - 2\cos(2\theta)| \right] \end{aligned} \tag{2.14}$$

where r_0 is a cutoff due to the expansion and $r^2(\theta)=x/(2t_2-2\cos(2\theta))$. The second part of the integration is finite as long as $\theta_0<\pi/4$, which corresponds to $t_2=0$, while the first part of the integration yields

$$\frac{2}{\pi^2} \int_0^{\theta_0} \frac{d\theta}{\cos(2\theta)} \left\{ \ln\left|\frac{r_0}{x}\right| = \frac{1}{\pi^2} \ln\left[\tan\left[\theta_0+\frac{\pi}{4}\right]\right] \ln\left|\frac{r_0}{x}\right| \right\} . \tag{2.15}$$

When $\mu \to -4t_2$, i.e., $x \to 0$, $\Gamma(\pi)$ diverges logarithmically with coefficient

$$\frac{1}{\pi^2} \ln\left[\tan\left[\theta_0+\frac{\pi}{4}\right]\right] .$$

On the other hand, the function $\Gamma(\mathbf{q})$ for the ferromagnetic state also diverges logarithmically at the Fermi level as $(1/\pi^2)\ln(1/x)$. Thus the ground state will be ferromagnetic if $1 > \ln[\tan(\theta_0+\pi/4)]$, i.e., $\tan(\theta_0) < \tanh(\frac{1}{2})$. Therefore the ferromagnetic state will be stable against the antiferromagnetic state when the next-nearest-neighbor interaction

$$t_2 \geq \cos(2\theta_0)/2 \geq \cos[2\tan^{-1}(\tanh(\tfrac{1}{2}))]/2 = \tfrac{1}{2}\cosh(1) = 0.324 .$$

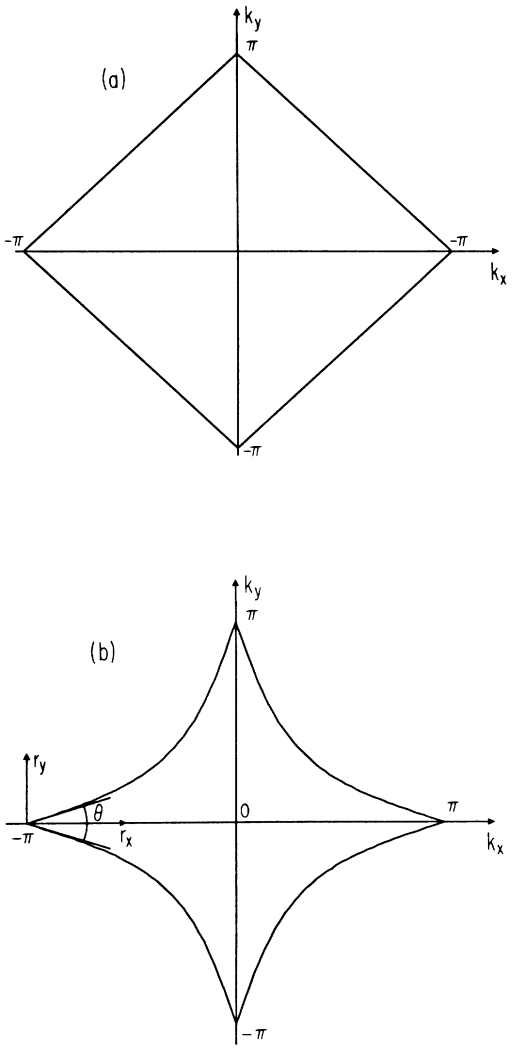

FIG. 2. The Fermi surfaces for different band filling and different next-nearest-neighbor hopping: (a) $t_2=0, \langle n \rangle = 1$; (b) $t_2=0.4$, $\mu=-4t_2$; (c) $t_2=0.2, \langle n \rangle = 1$.

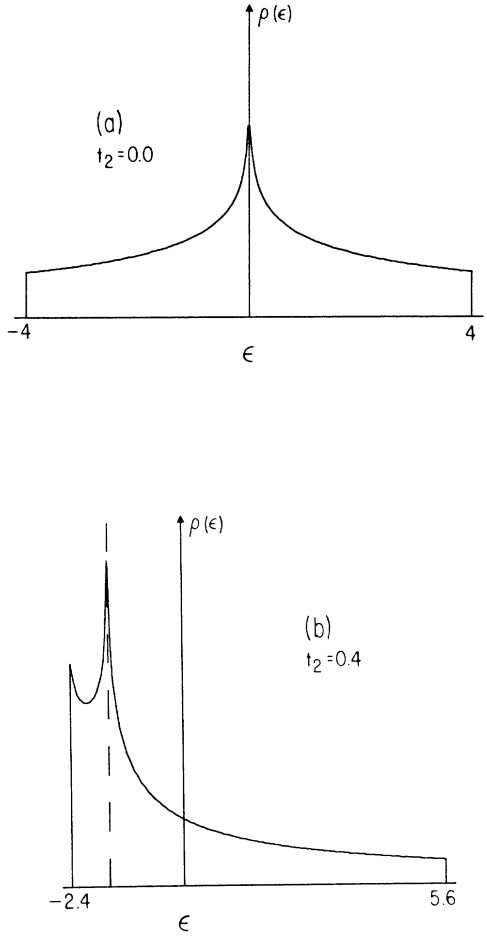

FIG. 3. The density of states for different hopping: (a) $t_2=0$, and (b) $t_2=0.4$.

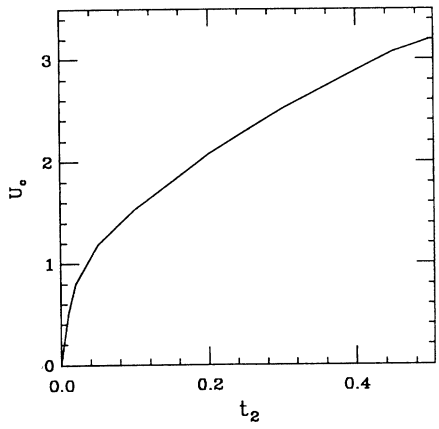

FIG. 4. Critical value U_c versus t_2 in HF calculations.

B. Paramagnetism versus antiferromagnetism at $n=1$

When $t_2=0$, Eq. (2.9b) reads

$$1=\frac{U}{N}\sum_{\{\mathbf{k}\}}\frac{1}{(e_{\mathbf{k}}^2+U^2m^2)^{1/2}}$$

$$=U\int_{-4t}^{0}d\epsilon\frac{\rho(\epsilon)}{(\epsilon^2+\Delta^2)^{1/2}},\quad \Delta\equiv Um\ , \tag{2.16}$$

which has a solution with $m\neq 0$ for arbitrarily small U due to the nesting of Fermi surface. When $t_2\neq 0$, we expect that there exists a nonzero value of U_c such that $m=0$ for $U<U_c$, because nesting of the Fermi surface is absent. Indeed, setting $m=0^+$ in Eq. (2.9b) we have

$$1=\frac{U_c}{N}\sum_{\{\mathbf{k}\}}\frac{f(E_{\mathbf{k}}^-)-f(E_{\mathbf{k}}^+)}{2\,|\,t\,|\,(\cos k_x+\cos k_y)}$$

$$=\frac{4U_c}{(2\pi)^2}\int_{D(\mathbf{k})}\frac{dk_x dk_y}{2\,|\,t\,|\,(\cos k_x+\cos k_y)}\ , \tag{2.17}$$

where we have used the fact that $\cos k_x+\cos k_y>0$ for $k_x+k_y<0$. The integration region $D(k)$ is determined by the condition: $E_k^+>0$, $E_k^-<0$, which is shown in Fig. 2(c). The singular points are marked there for which $\cos k_x+\cos k_y=0$. Expanding the integrand around these points we get, say, at point A's neighbor $A(\mathbf{k})$, to lowest order

$$\cos k_x+\cos k_y=-\sin k_x^0[(k_z-k_x^0)+(k_y-k_y^0)]$$
$$+O[(\mathbf{k}-\mathbf{k}^0)^2]\ . \tag{2.18}$$

Then Eq. (2.17) becomes, after a change of variables,

$$1=\frac{2U_c}{(2\pi)^2\,|\,t\,|}\left[\frac{8}{-\sin k_x^0}\int_{A(k)}\frac{dx\,dy}{x+y}+\text{normal part}\right]=\frac{2U_c}{(2\pi)^2\,|\,t\,|}\left[\frac{8}{-\sin k_x^0}\int_0^{r_0}\frac{r\,dr}{r}\int\frac{d\theta}{\sin\theta+\cos\theta}+\text{normal part}\right]$$

and we have

$$\int\frac{d\theta}{\sin\theta+\cos\theta}=\frac{1}{\sqrt{2}}\frac{d\theta}{\sin\left[\theta+\frac{\pi}{4}\right]}\ .$$

It is clear from Fig. 2(c) that $3\pi/4<\theta<7\pi/4$. Hence $\pi<\theta+\pi/4<2\pi$ and the integral is finite so $U_c\neq 0$. The critical value U_c predicted by the mean-field calculation as a function of t_2 is shown in Fig. 4, in particular, $U_c=2.1$ for $t_2=0.2$.

III. MONTE CARLO SIMULATIONS

We write the partition function as

$$Z=\mathrm{Tr}\{\exp(-\beta H)\}=\mathrm{Tr}\prod_{l=1}^{L}e^{-\Delta\tau H}$$

$$\approx\mathrm{Tr}\prod_{l=1}^{L}e^{-\Delta\tau H_0}\exp\left[-\Delta\tau\left[U\sum_i n_{i\uparrow}n_{i\downarrow}-\mu\sum_i(n_{i\uparrow}+n_{i\downarrow})\right]\right]\ , \tag{3.1}$$

where $\beta=L\Delta\tau$ and the error due to the breakup in Eq. (3.1) is of order $O(\Delta\tau^2 tU)$. Next we eliminate the electron-electron interaction term with a discrete Hubbard-Stratonovich transformation:[9]

$$\exp(-\Delta\tau U n_{i\uparrow}n_{i\downarrow})=\mathrm{Tr}_\sigma\exp\left[\lambda\sigma(n_{i\uparrow}-n_{i\downarrow})-\frac{\Delta\tau U}{2}(n_{i\uparrow}+n_{i\downarrow})\right]\ , \tag{3.2}$$

where σ are auxiliary Ising variables ($\sigma=\pm 1$) with coupling $\lambda=2\arctan\sqrt{\tanh(\Delta\tau U/4)}$. The partition function is then[10]

$$Z\approx\mathrm{Tr}_\sigma\mathrm{Tr}\prod_{l=1}^{L}e^{-\Delta\tau H_0}\exp\left[\lambda\sigma(n_{i\uparrow}-n_{i\downarrow})-\Delta\tau\left[\mu-\frac{U}{2}\right](n_{i\uparrow}+n_{i\downarrow})\right]$$

$$=\mathrm{Tr}_\sigma\mathrm{Tr}\prod_{\alpha=\pm}\prod_{l=1}^{L}e^{-\Delta\tau H_{0\alpha}}\exp\left\{\left[\alpha\lambda\sigma-\Delta\tau\left[\mu-\frac{U}{2}\right]\right]n_{i\alpha}\right\}$$

$$=\mathrm{Tr}_\sigma\prod_{\alpha=\pm}\det[I+B_L(\alpha)B_{L-1}(\alpha)\ldots B_1(\alpha)]=\mathrm{Tr}_\sigma\det O_\uparrow\det O_\downarrow\ , \tag{3.3}$$

where

$$B_l(\alpha)=e^{-\Delta\tau K}e^{V^{\alpha}(l)}, \tag{3.4a}$$

$$(K)_{ij}=\begin{cases}-t & \text{if } i,j \text{ are nearest neighbor}\\ t_2 & \text{if } i,j \text{ are next nearest neighbor}\\ 0 & \text{otherwise}\end{cases}, \tag{3.4b}$$

$$V_{ij}^{\alpha}(l)=\delta_{ij}\left[\lambda\alpha\sigma_i(l)-\Delta\tau\left[\mu-\frac{U}{2}\right]\right]. \tag{3.4c}$$

To sum over Ising spins in Eq. (3.3) we perform a Monte Carlo simulation with an appropriate Boltzmann weight. When $t_2=0$, the product of determinants $\det O_{\uparrow}\det O_{\downarrow}$ is positive for arbitrary $\{\sigma\}$ configurations in the case of a half-filled band because of particle-hole symmetry so we can take it as the Boltzmann weight $P(\sigma)$. For $t_2\neq 0$, however, the particle-hole symmetry is missing and the product $\det O_{\uparrow}\det O_{\downarrow}$ is not positive definite so we define the Boltzmann weight $P(\sigma)=|\det O_{\uparrow}\det O_{\downarrow}|$ and have to compute the average of the sign of the product of determinants. The simulation works as long as the average of the sign is not too small. In performing the simulation we use the heat-bath algorithm. We flip a given Ising spin with probability $P=R_{\uparrow}R_{\downarrow}/(1+R_{\uparrow}R_{\downarrow})$ where R_{σ} is the ratio of the new determinant to the old one. To compute R_{σ} we use the procedure introduced by Blankenbecler, Scalapino and Sugar.[10]

We have checked the reliability of our simulation program by comparing with exact results for a 2×2 lattice, as shown later, and by comparing with exact results for the noninteracting case with lattices up to 8×8 spatial sites. Other comparisons with exact results for two-site and six-site rings have been reported earlier.[8,9] It is found that the choice $\Delta\tau\sqrt{Ut}=0.25$ gives better than 5% accuracy for all quantities measured. Readers can find more detail about the present Monte Carlo algorithm in Refs. 8–11. Most of our simulations were performed on a Ridge 32 minicomputer. The computer time in this algorithm is proportional to LN^3, where N is the size of the system and L is the number of time slices ($L=\beta/\Delta\tau$). It takes about 1.5 min CPU time on the Ridge for a single Monte Carlo sweep at $\beta=3$, $L=48$ for a 4×4 lattice. A single data point usually involved about 2500 Monte Carlo sweeps.

As the lattice size increases and the temperature is lowered, the average of the sign of the product of determinants becomes smaller and the statistical error increases, especially so for $t_2\neq 0$ away from the half-filled band. As a consequence of this we were able to study up to 8×8 lattices with $t_2=0.2$ in the half-filled band sector, but only up to 6×6 lattices with $t_2=0.4$ and $n=0.67$. The statistical error in the figures is smaller than the points where not shown.

The question that we want to address is the existence of various kinds of magnetic long-range order. At finite temperature, the Hubbard model cannot have long-range order since it has continuous symmetry in spin space which cannot be broken in two dimensions. The system, however, can exhibit long-range magnetic order when $T=0$. Although our simulation method cannot deal with zero temperature directly, we can go to sufficiently low temperatures so that correlations build up over the whole lattice. When the thermal coherence length, $v_f\beta$ (v_f denotes Fermi velocity), is much larger than the spatial lattice size, the system behaves effectively as if at zero temperature. We investigate the magnetic structure of the system by studying the Fourier transform of the spin-spin correlation function

$$S(\mathbf{q})=\frac{1}{N}\sum_{i,j}e^{i\mathbf{q}\cdot(\mathbf{R}_i-\mathbf{R}_j)}\langle(n_{i\uparrow}-n_{i\downarrow})(n_{j\uparrow}-n_{j\downarrow})\rangle. \tag{3.5}$$

The largest $S(\mathbf{q})$ corresponds to the system attempting to form a spatially oscillating spin density of wavelength $\mathbf{q}$. $S(\mathbf{q}=\mathbf{0})$ corresponds to ferromagnetic spin alignment, and $S(\mathbf{q}=\boldsymbol{\pi})$ to antiferromagnetic alignment. For $\mathbf{q}=\mathbf{0}$, we have a relation between susceptibility χ and spin-spin correlation function:

$$\chi(\mathbf{q}=\mathbf{0})=\beta S(\mathbf{q}=\mathbf{0}) \tag{3.6}$$

since the total magnetization commutes with the Hamiltonian. For $\mathbf{q}=\boldsymbol{\pi}$, we will have for sufficiently large lattices at $T=0$:

$$S(\boldsymbol{\pi})=Nm^2+S_c(\boldsymbol{\pi}) \tag{3.7}$$

with m the staggered magnetization

$$m=\frac{1}{N}\sum_i(-1)^{i_x+i_y}\langle n_{i\uparrow}-n_{i\downarrow}\rangle \tag{3.8}$$

and S_c the connected structure factor. To extrapolate the long-range order, we plot $S(\boldsymbol{\pi})/N$ versus $1/N$ and expect $S(\boldsymbol{\pi})/N$ to follow a straight line for sufficiently large N according to Eq. (3.7). From the extrapolated value as $N\to\infty$, we obtain the square of the staggered magnetization m. To do so it is essential to consider finite lattices that can accommodate the Néel state using periodic boundary conditions, as pointed out by Oitmaa and Betts.[12] Such lattices with square cells in $d=2$ can be constructed for any number of sites N satisfying $N=r^2+s^2$, with r and s integers and $r+s$ even. We have done our simulations for lattices with $N=16$, 26, 36, 52, and 64. To scale the temperature with the lattice spatial size, we have taken $\beta=\gamma\sqrt{N}$. The factor γ is chosen to be 0.5, so that the lowest temperature studied was $\beta=4$ for $N=64$. This is about the lowest temperature so we could study without having accuracy problem in the computations.

Fig. 5(a) shows our results for $t_2=0.2$. For $U=2.0$, the points extrapolate to zero. The extrapolated value starts to be finite as $U\geq 2.5$, and it is clearly finite for $U=3.0$. We also show the results for $t_2=0$ in Fig. 5(b) for comparison. There the extrapolation is already finite for $U=2$. We estimate the transition value to be $U=2.5\pm 0.25$. The critical value of U estimated by the mean-field calculation in the preceding section is close to the one we get here ($U_c=2.1$). We also did some simulations for band filling $n=0.88$, which corresponds to $\mu=-4t_2$ with $t_2=0.2$ in the mean-field calculation. As we have shown in Sec. II, the Hartree-Fock ground state there is antiferromagnetic no matter how small the interaction U is. However, simulations show that antiferromagnetism becomes weaker away from the half-filled

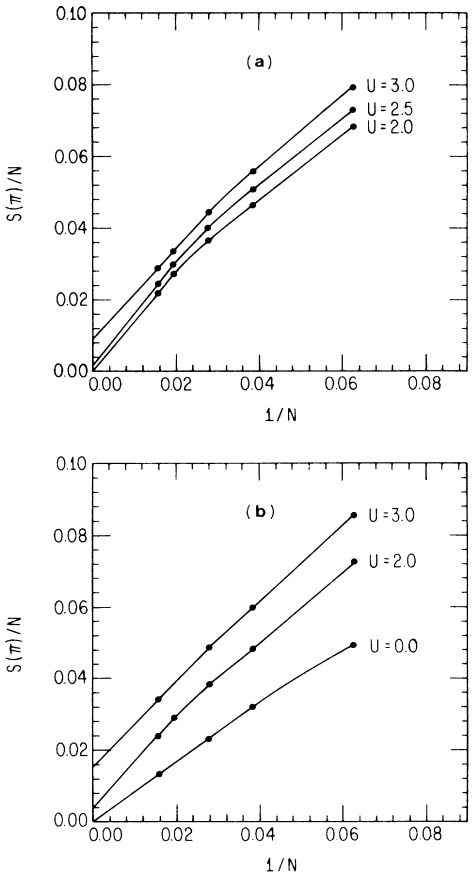

FIG. 5. Spin-spin correlation $S(\pi)/N$ versus $1/N$ for half-filled band: (a) $t_2=0.2$; (b) $t_2=0$.

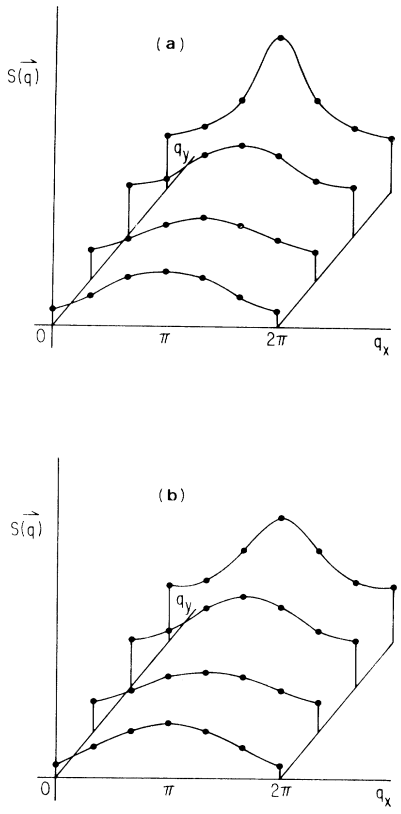

FIG. 6. Spin-spin correlation functions $S(\mathbf{q})$ for $U=2.5$ with band fillings (a) $n=1$ and (b) $n=0.88$, on a 6×6 lattice at $\beta=4.5$.

case. Figure 6 shows the behavior of the spin-spin correlation functions for $U=2.5$ with band fillings $n=1$ and $n=0.88$, for 6×6 lattice at $\beta=4.5$. Both peaks appear at (π,π) but the one for $n=1$ is higher than that of $n=0.88$. Since in the case of $t_2=0$ it was found[8] that there is no antiferromagnetic long-range order away from $N=1$, and antiferromagnetism is weakened by having $t_2\neq0$, we conclude that there is no antiferromagnetic order here either way from the half-filled band case.

IV. EXISTENCE OF FERROMAGNETISM

An interesting question is the existence of ferromagnetism in two dimensions for the Hubbard model. For the case of nearest-neighbor hopping only, ferromagnetism is predicted to occur for large values of U and band filling close to 0.67 in the Hartree-Fock scheme. The Monte Carlo simulations for this case, however, do not give any indication that there is a tendency towards ferromagnetic ordering up to $U=8$. Figure 7 shows the $\mathbf{q}=\mathbf{0}$ and $\mathbf{q}=\pi$ structure factors for $t_2=0$, band filling $n=0.67$ and $U=0,4$, and 8 as functions of temperature on a 6×6 lattice. The interaction U enhances both the antiferromagnetic and ferromagnetic correlations (and hence the sus-

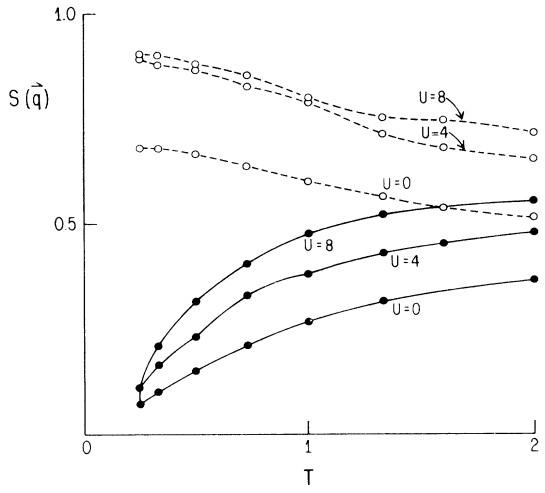

FIG. 7. Structure factor for $t_2=0$, band filling $n=0.67$ and $U=0$, 4, and 8 as functions of temperature on a 6×6 lattice, where the solid lines represent $\mathbf{q}=\mathbf{0}$, while the dashed lines represent $\mathbf{q}=\pi$.

ceptibility $\chi=\beta S$ ($q=0$). However, the $\mathbf{q}=\mathbf{0}$ structure factor is still suppressed as T goes to zero and in fact decreases more rapidly as U increases. Antiferromagnetic correlations are always larger but do not show a divergence either.

When we turn on a large enough next-nearest-neighbor hopping ($t_2>0.324$), the mean-field calculation (Sec. II) predicted that ferromagnetism would occur for arbitrary U at band filling corresponding to $\mu=-4t_2$. We studied this problem by starting with exactly diagonalizing a 2×2 lattice. Since the Hubbard Hamiltonian commutes with the total number of electrons N and the total spin S we can diagonalize $H(N,S)$ in that subspace. For the 2×2 lattice, the value $N=3$ corresponds to chemical potential up to $\mu=-4t_2$. The total spin S for $N=3$ has only two values, i.e., $\frac{3}{2}$ or $\frac{1}{2}$. Figure 8 shows the lowest eigenvalue in the lower-spin state ($S=\frac{1}{2}$) as a function of U and t_2 versus the totally ferromagnetic state ($S=\frac{3}{2}$). The state with $S=\frac{3}{2}$ does have lower energy than the state with $S=\frac{1}{2}$ when $U>4.6$ for $t_2=0.4$. For $t_2=0.2$ this happens at higher value of U ($U\geq8.48$), and for $t_2=0$ at $U\geq18$. So we see that ferromagnetism is enhanced by the next-nearest-neighbor hopping t_2, provided it is of the right sign. This effect has been recently discussed by Mattis and Pena[13] and by Takahashi.[14] We also show the behavior of spin-spin correlations $S(\mathbf{0})$ and $S(\pi)$ in Fig. 9 for different values of U at $t_2=0.4$. (Note the agreement

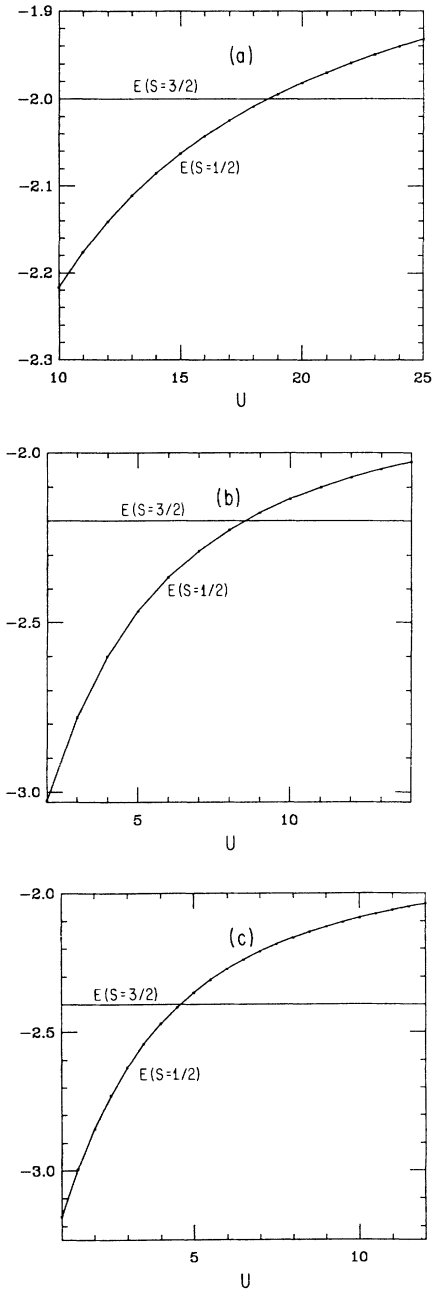

FIG. 8. The lowest eigenvalue in lower-spin state ($S=\frac{1}{2}$) as a function of U for (a) $t_2=0$, (b) $t_2=0.2$, and (c) $t_2=0.4$. The horizontal line corresponds to the ground-state energy of higher-spin state ($S=\frac{3}{2}$), i.e., ferromagnetic state.

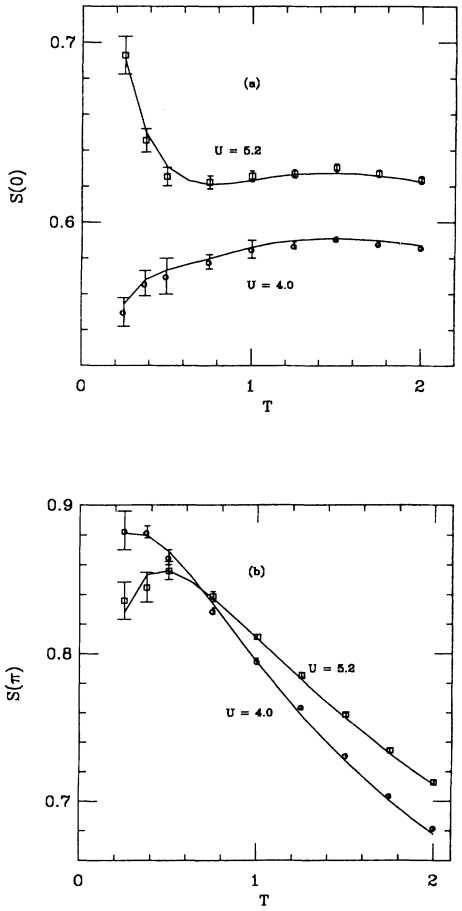

FIG. 9. Spin-spin correlation (a) $S(\mathbf{0})$, and (b) $S(\pi)$ for different values of U at $t_2=0.4$ on a 2×2 lattice from simulations (dots) and exact diagonalization (lines).

between Monte Carlo and exact diagonalization results.) The spin-spin correlation $S(\mathbf{0})$ decreases with decreasing temperature at lower temperature but $S(\pi)$ increases with decreasing temperature for $U=4$. For $U=5.2$, however, the behaviors of $S(\mathbf{0})$ and $S(\pi)$ are opposite to that of $U=4$. $S(\mathbf{0})$ does increase while $S(\pi)$ decreases with decreasing temperature as expected. Thus, the results for the spin-spin correlation functions are consistent with the energy calculations.

In Fig. 10 we show results of Monte Carlo simulations for 4×4 and 6×6 lattices at $U=8$ and band filling $n=0.67$, and compare them with results for 2×2 lattices. It can be seen that ferromagnetism is suppressed on the larger lattices as $T\rightarrow0$, while antiferromagnetism is enhanced. (This is the case for which HF predicts ferromagnetism down to $U=0$.) $S(0)$ is larger for the 6×6 lattice compared to the 4×4 lattice, but still decreases as T is lowered. If there existed finite ferromagnetic long-range order, $S(0)/N$ should extrapolate to a finite value. From Fig. 10, however, one finds that $S(0)/N$ becomes smaller as N increases. Thus, our results show that the critical value of U for ferromagnetism to occur on a 4×4 or 6×6 lattice is much larger than on the 2×2 lattice and than the HF prediction and suggest that there may not be ferromagnetism for any value of U on an infinite lattice.

V. CONCLUSIONS

We have studied magnetic properties of the two-dimensional Hubbard model with nearest- and next-nearest-neighbor hopping t and t_2. Since almost any modification of the nearest-neighbor hopping case will destroy the special feature of that case (nested Fermi surface), the present model is presumably a generic one. Within the Hartree-Fock approximation we discussed the nature of the phase diagram and the criterion for ferromagnetism or antiferromagnetism extending down to zero interaction. Although one may expect Hartree-Fock to give some qualitative features correctly, it cannot be trusted especially in less than three dimensions since it neglects fluctuations. For that reason, we studied the model numerically to assess the validity of the Hartree-Fock predictions.

The results in general disagree with Hartree-Fock calculations except in one case: for the half-filled band case, the numerical results suggest that a critical U exists for the appearance of antiferromagnetism. For the case $t_2=0.2$, it was estimated to be $U_c=2.5\pm0.25$, not too far from the HF prediction $U_c=2.1$. However, simulations show that antiferromagnetism decreases as one moves away from the half-filled band, while HF predicts antiferromagnetism to extend down to $U=0$ for other band fillings.

For the question of existence of ferromagnetism, we studied 2×2 lattices by exact diagonalization, and 4×4 and 6×6 lattices by Monte Carlo simulation. Our results show that the ferromagnetism found for the 2×2 case and predicted by Hartree-Fock, disappears in going to larger lattices. In other words, the critical U for the appearance of ferromagnetism for given parameters and band filling is a rapidly increasing function of lattice size.

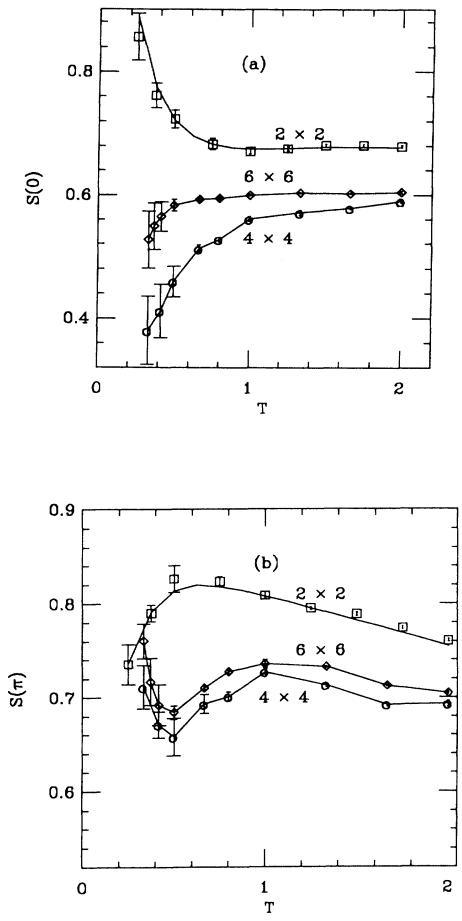

FIG. 10. Spin-spin correlation (a) $S(\mathbf{0})$, and (b) $S(\pi)$ at $U=8, t_2=0.4$ for 2×2, 4×4, and 6×6 lattices. For the 2×2 case the solid lines are exact results, in the other cases they are drawn through the Monte Carlo points to guide the eye.

Although we cannot extract definite answers for the thermodynamic limit, our results suggest that ferromagnetic long-range order probably does not occur in the two-dimensional Hubbard model even for "favorable" band structures like the one studied here. This is in disagreement with HF predictions but in agreement with a recent study by Rudin and Mattis.[15] We also expect the properties of a triangular lattice to be quite similar to the case discussed here.

ACKNOWLEDGMENTS

This work was supported by the National Science Foundation under Grant No. DMR-85-17756. J.H. is grateful to the A. P. Sloan Foundation for financial support.

[1]J. Hubbard, Proc. R. Soc. London, Ser. A **276**, 283 (1963); **281**, 401 (1964).
[2]See, for example, *Electron Correlation and Magnetism in Narrow-Band Systems*, edited by T. Moriya (Springer, New York, 1981), and references therein.
[3]M. C. Gutzwiller, Phys. Rev. Lett. **10**, 159 (1963); Phys. Rev. **137**, A1726 (1965).
[4]E. Lieb and F. Wu, Phys. Rev. Lett. **20**, 1445 (1968).
[5]D. Penn, Phys. Rev. **142**, 350 (1966).
[6]M. Cyrot, J. Phys. (Paris) **33**, 125 (1972); Phys. Lett. **A37**, 189 (1971).
[7]H. Shiba and P. Pincus, Phys. Rev. B **5**, 1966 (1972); H. Shiba, Prog. Theor. Phys. **48**, 2171 (1972).
[8]J. E. Hirsch, Phys. Rev. B **31**, 4403 (1985); Phys. Rev. Lett. **51**, 1900 (1983).
[9]J. E. Hirsch, Phys. Rev. B **28**, 4059 (1983).
[10]R. Blankenbecler, D. J. Scalapino, and R. L. Sugar, Phys. Rev. D **24**, 2278 (1981); D. J. Scalapino and R. L. Sugar, Phys. Rev. B **24**, 4295 (1981).
[11]J. Gubernatis, D. J. Scalapino, R. L. Sugar, and W. D. Toussaint, Phys. Rev. B **32**, 103 (1985).
[12]J. Oitmaa and D. Betts, Can. J. Phys. **56**, 897 (1978).
[13]D. C. Mattis and R. E. Pena, Phys. Rev. B **10**, 1006 (1974).
[14]M. Takahashi, J. Phys. Soc. Jpn. **51**, 3475 (1982).
[15]S. Rudin and D. C. Mattis (unpublished).